HEFAT2010
7th International Conference on Heat Transfer, Fluid Mechanics and Thermodynamics
19-21 July 2010
Antalya, Turkey

Thermal Joint Resistance of Solid Materials as a Function of Pressure and Roughness

Manaf A. Mahammed* , Khairi M-S Abdullah and Moayad A,Mohammed
*Author for correspondence
Department of Physics/College of Science.
University of Duhok,
Duhok,
Iraq,
E-mail: manafzivingy@yahoo.com

ABSTRACT

An analytical model was developed for predicting the thermal joint resistance of nonconforming rough surfaces in contact with the presence of air under atmospheric pressure as a TIM. Accordingly four models were developed in the present work.

The thermal macrocontact resistance was modeled for the transition case, with the existence of surface roughness and surface out of flatness.

The microcontact radius was modeled correlating the microcontact radius to the relative applied pressure, which was used with the thermal constriction parameter to develop an accurate nondimensional contact conductance and thermal microcontact resistance.

The thermal microgap resistance model is derived assuming the TIM is air under atmospheric pressure and taking into account the effect of surface curvature. The microgap resistance has the largest values among the other components, since the TIM which was air has very low thermal conductivity and a small microgap area.

The thermal macrogap resistance builds up in the region surrounding the macrocontact area which was also filled with air under atmospheric pressure as TIM.

Throughout the above analytical work it was assumed that the surface asperities deform plastically while the bulk material deform elastically as been assumed by almost the majority of the researchers in this field.

On the other hand and in order to support the present theoretical models, an experimental investigation was carried out to measure the thermal joint resistance for the contact of nonconforming rough surfaces with air under atmospheric pressure as a TIM. A laboratory experimental setup was designed and implemented. The examined contacting surfaces were aluminium and brass. Many surface processes were done comprising cutting, chemical cleaning, and ultrasonic cleaning. Also many geometrical and mechanical parameters were measured for the contacting samples that include, surface roughness, surface asperity slope, surface out-of-flatness, and material bulk hardness. Collected data are tabulated and the related equations were used to calculate the heat flux, temperature drop, and the thermal joint resistance, as well as their estimated error. The measured results were compared with the theoretical model mentioned above and a good agreement is observed.

The differential error estimated for the thermal joint resistance is ranged from (0.00248) to (0.00557) ^{0}C/w.

INTRODUCTION

A thermal joint is formed when two nonconforming rough surfaces are brought into contact under the effect of external applied force, with air under atmospheric pressure filling both microgaps and macrogap. As the thermal energy passes through the thermal joint, the air filling the interfacial region, the thermal and mechanical properties of contacting surfaces, as well as the topography of the contact plane due to surface roughness, asperity slope and out-of-flatness contribute to impede the heat transfer and cause a temperature drop ΔT_j across joint. This causes the formation of the thermal joint resistance R_j which is defined as the amount of temperature drop ΔT_j across the joint divided by the amount of heat flux Q_j passing through the joint.

$$R_j = \Delta T_j / Q_j \quad (1)$$

and the thermal joint conductance can be written as

$$h_j = Q_j/(\Delta T_j A_j) \quad (2)$$

where A_j is the total joint contact area.

Analytical models for thermal joint resistances are available for idealized surface geometries, including conforming rough surfaces and nonconforming smooth surfaces. These models are typically not realized the real surfaces that combine both surface roughness and waviness especially for interfaces that incorporate interstitial materials to promote compliance [1].

The problem to be solved is to predict the thermal joint resistance of real contacting engineering surfaces. Analytical model is to be deduced to calculate the thermal joint resistance of joints composed of real surfaces having a combination of surface roughness, asperity slope, surface out-of-flatness with the existence of air under standard atmospheric pressure filling the gap.

The contact of two rough metallic surfaces is considered conforming rough surfaces when the nonuniformity of the contact is very little and can be neglected. Of course, there is no real engineering surface free of nonuniformity on the

macroscopic scale and they are not perfectly flat. So the out of flatness of engineering surfaces can never be ignored [2]. The waviness or out-of flatness in the engineering surfaces is also known as macroscopic topography of the surface.Many simplifications were used by researchers to defeat these difficulties and to reduce the problem into a simple manner of few variables.

According to Johnson [2], in static frictionless contact of solids, the contact stresses depend only on the relative profile of the two surfaces, i.e., on the shape of the interstitial gap before loading. Hertz [2], replaced the two surface contact geometry by a flat surface and a profile, which results of the same undeformed gap between the surfaces. Also, due to the application of external load, the elastic deformation occurs to both surfaces. For simplicity, all elastic deformation is considered to occur only in a body of flat surface, and the effective elastic modulus that is given by the following relation:

$$\frac{1}{E'} = \frac{1-\upsilon_1^2}{E_1} + \frac{1-\upsilon_2^2}{E_2} \quad (3)$$

where E_1, ν_1 are respectively the Yong modulus and Poisson ratio of surface 1 and E_2 , $\nu_2$are respectively that of surface 2. Hertz derived a relationship for the radius of contact area known as Hertz radius a_H given by:

$$a_H = \left(\frac{3F\rho}{4E}\right)^{\frac{1}{3}} \quad (4)$$

where the effective radius of curvature of the two surfaces ρis given by the following relation [2]:

$$\rho = \frac{\rho_1\rho_2}{\rho_1+\rho_2} \quad (5)$$

where ρ_1 and ρ_2 are the equivalent radii of curvature of both surfaces 1 and 2 respectively.

According to the theoretical approaches by Clausing and Chao [3], Mikic and Rohsenow [4], Yovanovich [5], Nishino et al.[6], Lambert and Fletcher [7] and Bahrami et al.[8], the spherical profile might approximate the shape of the macroscopic nonuniformity and due to Lambert [9] this assumption is justifiable because nominally flat engineering surfaces are often spherical, or crowned (convex), with very large radius of curvature. The approximate relationship between the radius of curvature and the maximum out-of-flatness, for relatively large radii of curvature (approaching flat) [8, 3] is:

$$\rho = \frac{b_L^2}{2\delta} \quad (6)$$

where δ is the maximum out-of-flatness of the surface and b_L is the cylindrical body radius.

Microhardness depends on several parameters; surface roughness, slope of asperities, method of surface preparation and applied pressure. Song and Yovanovich [10], related the contact microhardness to the surface parameters and nominal pressure:

$$\frac{P}{H_{mic}} = \left[\frac{P}{c_1(1.62\frac{\sigma'}{m})^{c_2}}\right]^{\frac{1}{(1+0.71c_2)}} \quad (7)$$

Sridhar and Yovanovich [11], suggested an empirical relations to estimate the Vickers microhardness coefficients given by Hegazy empirical equation (2.18) by using the bulk hardness of material:

$C_1=H_{BGM}(4.0\text{-}5.77K+4.0K^2\text{-}0.61K^3)$

$C_2=\text{-}0.57+0.825K\text{-}0.41K^2+0.06K^3$

$K=H_B/H_{BGM}$

NOMENCLATURE

A = area, m^2.
a = mean microcontact radius, m.
A_a = apparent contact area, m^2.
$A_a = A_r + A_g$, m^2
A_g = microgap area, m^2
A_G = macrogap region area, m^2.
a_H = Hertzian contact radius, m.
A_j = thermal joint area, m^2.
a_L = macrocontact radius, m.
A_r = real contact area, m^2.
a_s = microcontact radius, m.
b = flux tube radius, m.
b_L = contacting bodies radius, m.
b_s = flux tube radius associated to the microcontact, m
$C = Mb_L^2/\delta$
C_1 = Vickers microhardness coefficient, GPa.
C_2 = Vickers microhardness coefficient.
E' = equivalent modulus of elasticity, Pa.
E_1 = Young modulus of surface 1, Pa.
E_2 = Yonug modulus of surface 2, Pa.
erfc (z) = complementary error function.
F = applied force, N.
F(z) = Gaussian distribution function.
H_{BGM} = 3.178 GPa
H_c = contact microhardness, Pa.
h_g = gap conductance, $w/m^2.^0C$.
h_j = thermal joint conductance, $w/m^2.^0C$.
H_{mic}= effective microhardness, Pa.
h_s =.thermal contact conductance, $w/m^2.^0C$.
H_v = Vickers microhardness, Pa.
$J_1(\delta_n)$ = Bessel function of the δ_n first kind of order one.
$K = H_B/H_{BGM}$
k = thermal conductivity, $w/m.^0c$.
k_1 = thermal conductivity of surface 1, $w/m.^0c$
k_2 = thermal conductivity of surface 2, $w/m.^0c$.
k_g = thermal conductivity of air or thermal grease, $w/m.^0c$
k_s = harmonic thermal conductivity of two materials in contact,
$w/m.^0c$
L = roughness stylus sampling length, m.
$L^2 = (a_L^2 - r^2)$
m' = average asperity slope.
M = gap parameter , m.
m = rms of asperity slope.
m_1 = rms of asperity slope of surface 1.
m_2 = rms of asperity slope of surface 2.
n_s = number of microcontacts.
P (r) = pressure as a function of r, Pa.
P = applied pressure, Pa.

$P(r/a_L)$ = general pressure distribution, Pa.
P_0 = maximum contact pressure, Pa.
$P_{0,H}$ = maximum Hertzian contact pressure, Pa.
p_g = gas (air) pressure, Pa.
P_m = mean apparent contact pressure, Pa.
Pr = Prandtl number.
Q = heat flow rate, w.
Q_G = heat transfer rate through the thermal macrogap area, w..
Q_j = heat transfer rate through the thermal joint, w.
r = distance from the center of the contact plane, m.
R_a = average roughness, m
R_G = thermal macrogap resistance, ^{0}C/w.
R_g = thermal microgap resistance, ^{0}C/w.
R_J = thermal joint resistance, ^{0}C/w.
r_j = specific joint resistance, m^2.k/kw.
$R_{j,EC}$ = elastoconstriction resistance, ^{0}C / w.
R_L = thermal macrocontact resistance, ^{0}C / w.
$R_{L,1}$ = macroconstriction resistance, ^{0}C/w.
R_{L2} = macrospreading resistance, ^{0}C/w.
$R_{material}$ = resistance due to conduction in the material, ^{0}C/w.
$R_{mic,\ flux\ tube}$ = constriction (spreading) resistance of flux tube, C / w.
R_s = thermal microcontact resistance, ^{0}C / w.
R_{si} = thermal resistance of the heat in passing one contact spot, ^{0}C/w.
R_{si1} = micro thermal constriction resistance, ^{0}C/w.
R_{si2} = micro thermal spreading resistance, ^{0}C/w.
R_{tube} = thermal resistance between the contact area and an arbitrary plane.
S = conduction shape factor. m
S_1 = conduction shape factor of surface 1.
S_2 = conduction shape factor of surface 2.
T = temperature, ^{0}C.
T_1, T_2 = temperature of both surfaces 1 and 2, or source and sink temperatures respectively.
TCR = thermal contact resistance.
T_g = air temperature, ^{0}C.
$W = 1.53\sigma\ (a_L.H_c/P_0)^{0.097}$
x = distance in the x- direction, m.
Y', Y = (used interchangeably), average effective distance between contacting bodies surfaces, or gap thickness, m.

Greek letters:

ΔT_G = temperature drop across the thermal macrogap, ^{0}C.
ΔT_j = temperature drop across the joint, ^{0}C.
δ = maximum out-of-flatness, m.
δ_1 = maximum out-of-flatness of surface 1, m.
δ_2 = maximum out-of-flatness of surface 2, m.
$\varepsilon = a_s/b_s$
$\lambda = \frac{Y}{\sigma}$, (relative mean plane separation).
ν_1 = Poisson ratio of surface 1.
ν_2= Poisson ratio of surface 2.
ρ =effective equivalent radius of curvature of two spherical profiles in contact,
ρ_1 = equivalent radius of curvature of surface 1, m.
ρ_2 = equivalent radius of curvature of surface 2, m.
$\sigma' = \sigma / \sigma_0$, $\sigma_0 = 1$ μm.
σ_1= surface roughness of surface 1, m.
σ = equivalent surface roughness of two surfaces in contact, m.
σ =standard deviation of roughness for conforming rough surfaces, m.
σ_2 = surface roughness of surface 2, m.
ψ_{si1} = thermal constriction factor of surface 1.
ψ_{si2} = thermal constriction factor of surface 2.
ψ = dimensionless spreading of half space.

where, H_B is the Brinell hardness of the bulk material, and H_{BGM} =3.178GPa.These correlations valid for the range $1.3 \le H_B \le 7.6$ GPa. The rms percent difference between data and calculated values of C_1 and C_2 were reported: 5.3% and 20.8%for C_1 and C_2 respectively [Bahrami, 2004].

Milanez et al.[Milanez et al, 2004], concluded that despite the difference between the measured data and the estimated values of microhardness coefficients, the TCR predicted by both methods are in good agreement.

The contact model of Cooper et al [14], which is known as CMY model, assumes that one of the contacting surfaces is softer and the deformation is purely plastic whether the harder asperities "penetrate" the softer metal, or whether the softer asperities are "flattened". There is a contact microhardness H_C, that can be assigned to the deformation of the contacting asperities. For the plastic deformation, the contact geometry parameters [14, 15]

$$\frac{A_r}{A_a} = \frac{1}{2}\operatorname{erfc}\left(\frac{\lambda}{\sqrt{2}}\right) \quad (9)$$

$$a = \sqrt{\frac{8}{\pi}}\left(\frac{\sigma}{m}\right)\exp\left(\frac{\lambda^2}{2}\right)\operatorname{erfc}\left(\frac{\lambda}{\sqrt{2}}\right) \quad (10)$$

If the joint operates in air, or any other gaseous environment, an estimate of the gap conductance can be made using a model proposed by Yovanovich [16]:

$$h_g = \frac{k_g}{Y' + M} \quad (11)$$

where the distance between the mean planes of the contacting surfaces is obtained from [17];

$$Y' = 1.53\sigma(P/H')^{-0.097} \quad (12)$$

The gas parameter M. For air at 377k and 1atm, M = 0.81μm and the thermal conductivity is k_g=0.0305 w/m.c [16]. Utilizing the Maxwell's theory for interfacial temperature discontinuity, Yovanovich et al. [18] proposed the following expression for the heat flux through a gas layer between two parallel plates for all four gas regimes:

$$q_g = \frac{k_g}{Y + M}(T_1 + T_2) \quad (13)$$

where q_g is the heat flux, $T_1$and T_2 are the temperatures of both the parallel plates 1 and 2 respectively, k_g is the thermal conductivity and M is the gas parameter.

MODELING OF THERMAL MACROCONTACT RESISTANCE

Cooper et. al.[14] proposed a simple accurate correlation for determining the flux tube constriction / spreading resistance:

$$R_{mic,flux\ tube} = \frac{\psi(\varepsilon_s)}{2k_s a_s} \quad (14)$$

where $\psi(\varepsilon_s) = (1-\varepsilon_s)^{1.5}$ and $\varepsilon_s = a_s/b_s$.

Using the flux tube correlation above, and neglecting the effect of surface roughness, the joint resistance for the smooth sphere-flat contact "elastoconstriction limit" can be determined by [19]:

$$R_{j,EC} = \frac{(1-a_H/b_L)^{1.5}}{2k_s a_H} \quad (15)$$

where a_H is the Hertz contact radius given by equation (**4**). The comparison between the elastoconstriction model (the above equation), and the smooth sphere-flat experimental data, shows good agreement [20]. Thus the flux tube solution can be employed for determining the thermal macroresistance

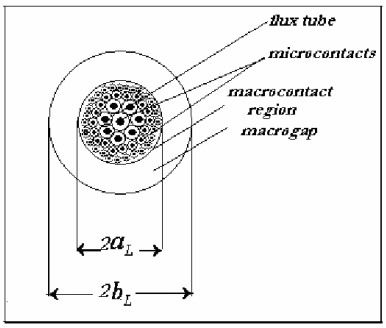

Figure 1 The contact plane between two modeled nonconforming rough surfaces

For the present work, when the heat flows from a heat source at T_1 to a heat sink at T_2, it experiences the macrothermal constriction causing the resistance $R_{L,1}$ which arose due to the macrocontact area and then the heat is passed through n_s parallel microcontacts in the contact plane causing the microcontact resistance R_s which will be shown in the subsequent section. After that, and also due to the macrocontact area, the heat experiences the macrothermal spreading causing the resistance $R_{L,2}$. Therefore, the total thermal contact resistance (TCR) of the contact of two non conforming rough surfaces in a vacuum (that has no interstitial material in the gap) can be written as the summation of the thermal macroresistance R_L and the microresistance R_s:

$$R_c = R_L + R_s \quad (16)$$

where $R_L = R_{L,1} + R_{L,2}$.

Considering the above equation, it can be noticed that the TCR ranges from the conforming rough limit (in which R_s is dominant) to elastoconstriction limit (in which R_L is dominant) passing through the transition region (in which both of R_s and R_L exist) .

According to Bahrami et. al.[19], the radius of the macrocontact area is given by the following relation:

$$a_L = 1.80 a_H \frac{\sqrt{a + 0.31\tau^{0.056}}}{\tau^{0.028}} \quad (17)$$

In the above equation, $\alpha = \sigma\rho/\alpha_H^2$, $\tau = \rho/a_H$. For very smooth surfaces in contact, $\sigma \to 0$, then $\alpha \to 0$, and $a_L = a_H$ which means that the macrocontact radius reduces to the Hertz radius which is the elastoconstriction limit. As the surface radius of curvature ρ decreases, the thermal joint resistance increases, which has been shown by experiments [19]. This increase is due to the formation of the macrocontact area and consequently the macrothermal resistance R_L. Thus the macrothermal resistance can be given by [8]:

$$R_L = \frac{(1-a_L/a_H)^{1.5}}{2k_s a_L} \quad (18)$$

and that this is in series with the thermal constriction resistance R_s when the contact is in vacuum,i.e., ($R_g = \infty$).

MODELING OF THERMAL MICROCONTACT RESISTANCE

Thermal Constriction (Spreading) Resistance:

Microcontacts are formed due to the contact of the higher asperities of both surfaces in contact under the application of an external force. When heat passes across the microcontact spots that are formed due to the contact of two metallic surfaces, the heat is constricted as it passes from the wide region to a narrower one and then it spreads as it passes from the narrow region to a wider one. The heat will suffer constriction and spreading resistances. Accordingly, the total resistance of the heat R_{si} in passing one contact spot (i^{th} microcontact) will be the result of two resistances in series:

$$R_{si} = R_{si1} + R_{si2} \quad (19)$$

where R_{si1} and R_{si2} are respectively the thermal constriction and spreading resistances of the i^{th} microcontact. The constriction (or spreading) resistance can be given by,

$$R_s = \psi_s / Sk \quad (20)$$

Therefore, the total constriction and spreading resistance of the i^{th} microcontact R_{si} can be given as:

$$R_{si} = \frac{\psi_{si1}}{s_1 k_1} + \frac{\psi_{si2}}{s_2 k_2} \quad (21)$$

Due to the geometrical and thermal symmetry about the contact plane [16], it can be resulted that $S_1 = S_2 = S$, $\psi_{si1} = \psi_{si2} = \psi_{si}$ and by assuming the microcontact as an isothermal surface of temperature T_1 and a semi-infinite medium of uniform temperature T_2 at a location well far from the surface , then S can be given by S=4a [21] where a is the mean microcontact radius. Then R_{si} can be written as $R_{si} = \psi_{si}/(2k_s a_i)$ where $k_s = 2k_1k_2/(k_1+k_2)$ is the harmonic thermal conductivity of both surfaces in contact [16].

Total constriction resistance due to n_s microcontacts that are assumed to be connected in parallel is given by:

$$\frac{1}{R_s} = \sum_{i=1}^{n_s} \frac{1}{R_{si}} \quad (22)$$

Assuming all microcontacts have the same mean radius a, then:

$$R_S = \psi_S / (2k_s n_s a) \quad (23)$$

According to equation (**10**), the mean microcontact radius a is related to the relative mean plane separation, Y/σ, through a very complex expression given by Mikic [15]. This expression contains a nonmeasurable quantity Y which is the mean plane separation between the two surfaces in contact. The mean plane separation, Y, is related to the relative contact pressure (P/Hc), by the relation [16]:

$$Y/\sigma = \sqrt{2}\ \mathrm{erfc}^{-1}(2P/H_c) \quad (24)$$

where $\mathrm{erfc}^{-1}(.)$ is known as the inverse complementary error function, The relative contact pressure (P/Hc) is defined as the ratio of the apparent applied pressure to the contact microhardness. Assuming plastic deformation of asperities and using equations (**10**) and (**24**), the relative microcontact radius a/(σ/m) is written as:

$$a/(\sigma/m) = (8/\pi)^{0.5} \exp[(\mathrm{erfc}^{-1}(2P/H_C))^2].(2P/H_C) \quad (25)$$

From equation (**24**), the relative gap thickness (mean plane separation) (Y/σ) is computed for the range of the relative contact pressure ($10^{-6} \le P/H_c \le 10^{-2}$), and substitute it into equation (**10**) which is the exact expression for the relative microcontact radius, the computations for the microcontact radius from this equation are done using the MATLAB program. The results of computation were used to find the following simple power correlation between the the relative microcontact radius and the relative gap thickness using EXCEL program:

$$a/(\sigma/m) = 0.96966(Y/\sigma)^{-0.835321} \quad (26)$$

From the above power correlation, it seems clear that, as the gap thickness Y is decreased by the application of an external pressure upon the two contacted surfaces, the microcontact radius increases. In order to have a simple correlation for the relative microcontact radius in terms of the relative contact pressure, the accurate approximation given by Song and Yovanovich [10] for the inverse complementary error function can be used:

$$\mathrm{erfc}^{-1}(2P/H_c) = 0.9638[-\ln(5.589P/H_c)]^{1/2} \quad (27)$$

and substitute it into equation (3.20):

$$Y/\sigma = \sqrt{2}\ [0.9638\{-\ln((5.589P/H_c)\}^{0.5} \quad (28)$$

Using both equations (**26**) and (26) and making further simplification will lead to the following simple and accurate expression instead of the complex expression given by equation (**25**):

$$a/(\sigma/m) = \{\ln(0.032/(P/H_c)^2\}^{-0.4176} \quad (29)$$

The correlation above, the exact expression of equation (**25**) and also the two correlations given by

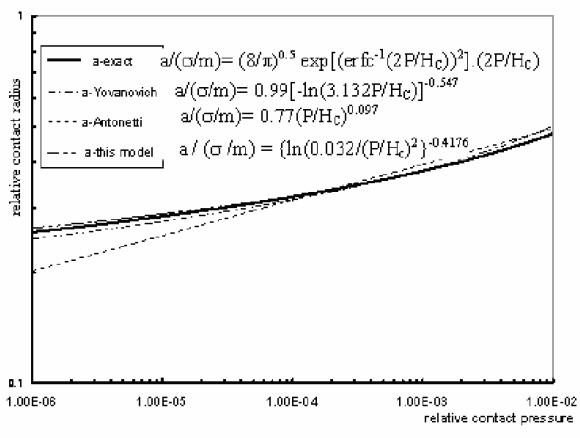

Figure 2 Comparison of microcontact radius models with the exact expression

Yovanovich [16] and Antonetti [17] are plotted in **figure 2**.The total range used for the relative contact pressure is ($10^{-6} \le P/H_c \le 10^{-2}$). The plot is avery good examination of the validity of the modeling of the relative microcontact radius given by equation (**9**).

In order to substitute for ψ_s in the thermal constriction resistance of equation (**23**), the following expression [22] is used in the present work:

$$\varepsilon = 1 - 1.4098\,\varepsilon + 0.3441\,\varepsilon^3 + 0.04\,\varepsilon\,3^5 + 0.0227\,\varepsilon^7 \quad (30)$$

where $\varepsilon = a/b = (A_r/A_a)^{1/2} = (P/H_c)^{1/2}$

Thermal Contact Conductance

The thermal contact conductance is related to the thermal constriction resistance as (equations **1,2**):

$$h_s = 1/(R_s A_a \quad (31)$$

where R_s is the total constriction (spreading) resistance and A_a is the apparent (nominal) contacting area.

Substituting for R_s from equation (**23**) into equation (**31**) we get:

$$h_s = 2k_s n_s\, a/(A_a \psi_c \quad (32)$$

Assuming plastic deformation mode, the ratio of the real contacting area to the apparent contact area is equal to the relative contact pressure, and the apparent contacting area can be written as:

$$A_a = A_r/(P/H_c \quad (33)$$

and the real contact area can be written as:

$$A_r = \pi\, n_s a^2 \quad (34)$$

From equations (**32**), (**33**) and (**34**) the thermal contact conductance h_s can be written as:

$$h_s = 2k_s(P/H_c)/(\pi\psi_s a) \quad (35)$$

Substituting for the microcontact radius a from equation (**29**) and the thermal constriction parameterψ_s from equation (**30**) into equation (35) and nondimensionalizing. The nondimensionalized thermal contact conductance ($h_c\sigma/k_s m$) is correlated to the relative contact pressure P/H_c for the range ($10^{-6} \le P/H_c \le 10^{-2}$) which is used for the most

practical purposes. MATLAB (v6.5) and EXCEL programs were used, as follows:

$$h_c\sigma/k_s m = 1.1942(P/H_c)^{0.9438} \quad (36)$$

The microcontact resistance from equation (**36**) can be written as:

$$R_s = 0.2665(\sigma / m\, k_s b_L^{\,2})(P/H_c)^{-0.9438} \quad (37)$$

This is the modeled thermal microcontact resistance and it forms an important component of the thermal joint resistance.

MODELING OF THERMAL MICROGAP RESISTANCE

The microgap resistance in the present work exists due to the impedance caused by the interfacial material to the heat transferring across the microgap. The microgap area A_g represents the majority of the macrocontact area even the individual microgap is the surrounding area to the corresponding microcontact area, since $A_c = A_r + A_g$ and that A_r/ A_c % ~ (1-2) %. then $A_g \sim A_c$.

Dividing the microgap area into infinitesimal parts each of elemental area equal to $dA_g = 2\pi r\, dr$ such that the heat transfer across each microgap element corresponding to area dA_g is the same as that of the gap between two conforming rough surfaces in contact. From equation (**11**), the total heat flux passing through the microgap is given by:

$$Q_g = \iint_{A_2} \frac{k_g(T_1 - T_2)}{Y(r) + M} dA_g \quad (38)$$

Substituting for dA_g and taking into consideration that r varies from (r = 0) which is the center of the microgap region to ($r = a_L$), then:

$$Q_g = 2\pi k_g(T_1\text{-}T_2) \int_0^{a_L} \frac{rdr}{Y(r) + M} \quad (39)$$

The microgap resistance can be written as:

$$R_g = (T_1\text{-}T_2)/ Q_g \quad (40)$$

Substituting for Q_g from equation (3.45),

$$R_g = (1/2\,\pi\, k_g)\{ \int_0^{a_L} \frac{rdr}{Y(r) + M} \}^{-1} \quad (41)$$

In order to find the microgap resistance in the equation above, it is necessary to substitute for Y(r) in terms of the distance r from the center of the contact plane.

For the case of two conforming rough surfaces in contact, Antonetti and Yovanovich [17] gave an expression for the gap thickness Y in terms of the relative contact pressure P/H_c as given by equation (**12**) in which the gap thickness Y is independent of the distance r from the center of the contact plane. Choosing a narrow ring of thickness dr from the macrocontact region such that the above equation holds right, then substituting for Y in equation (**12**), then equation (3.47) can be written as:

$$R_g = (1/2\pi k_g)\{ \int_0^{a_L} \frac{rdr}{1.53[P(r)H_c]^{-0097} + M} \}^{-1} \quad (42)$$

Bahrami et. al [23], derived an expression for the general pressure distribution in terms of the dimensionless radial position for the two nonconforming rough surfaces as $P(r/a_L) = P_0\,[1-(r/a_L)^2]^{\gamma}$, where, P_0 is the maximum pressure and is given by $P_0 = P_{0,H}\ /(1+1.37\alpha\tau^{-0.075})$, $P_{0,H}$ is the maximum Hertzian contact pressure and is given by

$P_{0,H} = 1.5F/\pi a_H^{\,2}$,

γ is the general pressure distribution exponent and is given by $\gamma = 1.5(P_0 / P_{0,H})(a_L / a_H)^2\text{-}1$and τ is a nondimensional parameter given by $\tau = \rho/a_H = (4E'\rho^2/3F)^{1/3}$

A good value given by Bahrami et. al.[23] for γ is 0.5. Then R_g can be written as:

$$R_g = \frac{W}{2\pi k_g}[\int_0^{a_L} \frac{rdr}{\left(a_L^2 - r^2\right)^{-0.0485} + \frac{M}{W}}]^{-1} \quad (43)$$

where $W = 1.53\sigma\,(a_L.H_c/P_0)^{0.097}$. Assuming $L^2 = (a_L^{\,2} - r^2)$, the equation of R_g can be written as:

$$R_g = \frac{M}{2\pi k_g}[\int_0^{a_L} \frac{L^{1.097}dL}{L^{1.07} + \frac{M}{W}}]^{-1} \quad (44)$$

The microhardness H_c in W can be substituted with the expression given by Hegazy [24], as:

$$H_c = (12.2\text{-}3.54H_b)(\sigma/m)^{-0.26} \quad (45)$$

and H_b is the bulk hardness of the softer material.

In equation (**44**) above the microgap thermal resistance can be determined when the integration inside the two brackets is found. The integration can be written as:

$$F = \int_0^{a_L} \frac{L^{1.097}dL}{L^{1.07} + \frac{M}{W}} \quad (46)$$

The integration above can be solved using Simpson Rule of integration for a range of applied force F and equation (**44**) will be:

$$R_g = M / (2\pi\, k_g F) \quad (47)$$

MODELING OF THE CONDUCTION MACROGAP RESISTANCE

The geometrical modeling of the macrogap thermal resistance is shown in **figure 3**. The macrogap region represents the noncontacting portion of the total contacting area outside the macrocontact region. The macrogap thickness Y(r) varies from zero at ($r = a_L$) to δ at ($r = b_L$). The maximum value of macrogap thickness represents the

summation of the maximum out-of-flatness of both surfaces in contact $\delta = \delta_{max1} + \delta_{max2}$ which can be given by $\delta = b_L^2 / 2\rho$. By using the same procedures made by Yovanovich [25], the macrogap region between the two surfaces is divided into infinitesimal surface elements each of thickness dr, and then the total heat flow through the macrogap region from the source of temperature T_1 to the sink of temperature T_2 is given by:

$$Q_G = \int_{a_L}^{b_L} \frac{k_g \Delta T_G}{Y(r) + M} dA \qquad (48)$$

Where $\Delta T_G = T_1 - T_2$, $dA_G = 2\pi r dr$

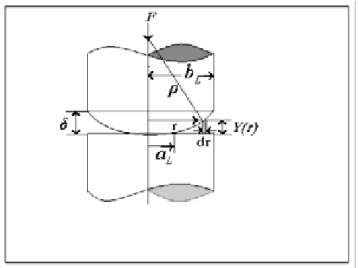

Figure 3 Geometrical modeling of the macrogap thermal resistance.

and Y(r) is the height of the infinitesimalelement and can be written as $Y(r) = \delta\, r^2/b_L^2$ where δ is the maximum out of flatness, r the distance from the center and b_L is the radius the contacting bodies. And the distance r varies in the range:

$$a_L \le r \le b_L$$

Substituting for Y(r) into equation (**48**), and using the relation $R_G = \Delta T_G / Q_G$, the macrogap resistance will be:

$$R_G = \frac{\delta}{\pi b_L^2 k_g} \left[\ln \frac{b_L^2 + C}{a_L^2 + C}\right]^{-1} \qquad (49)$$

Which is the same result given by Yovanovich [25].

Total equivalent thermal joint resistance:

In the preceding sections, the different four thermal resistances participating in the construction of the whole joint resistance were modeled geometrically, mechanically, and thermally. These resistances were the thermal macrocontact resistance R_L (equation **18**), microcontact resistance R_s (equation **37**), thermal microgap resistance R_g (equation **47**), and the thermal macrogap resistance R_G (equation **49**). These four thermal joint resistance components are assumed according to the present model to be connected as shown in **figure 4**. Accordingly, the equivalent thermal joint resistance R_J is given by the following expression:

$$R_J = \left[\frac{1}{R_G} + \frac{1}{R_L + \frac{R_s R_g}{R_s + R_g}}\right]^{-1} \qquad (50)$$

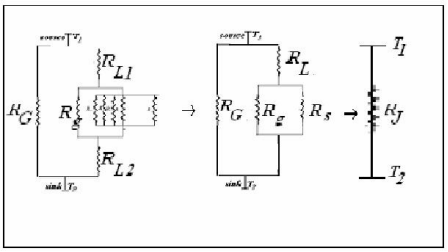

Figure 4 Equivalent thermal joint resistance and it components.

EXPERIMENTAL SETUP

The schematic diagram of the set up used in this work is shown in **figure 5,** while the photographic picture of the experimental set up is shown in **figure 6**. The set up consists of the metallic frame that holds all parts of the linear heat conduction section, the loading system and load measurement system. The metallic frame consists of lower square end upon which a fixed supporting base plate of thickness 40 mm is settled. Two vertical supporting bars are fixed between this plate and the upper end of the metallic frame. There is a movable sliding plate with the same dimension of the above plate that can be moved up and down on the two vertical supporting bars.

The loading system consists of a hydraulic jack (4) mounted on the movable sliding plate (5) and there is a helical spring inside the pipe (2) that is fixed on the top of the metallic frame. The linear heat conduction section is mounted on the load cell (9) which is in turn mounted on the supporting base plate (10). As the hydraulic jack is loaded, the helical spring is compressed and a force is applied on the linear thermal conduction section through the moving down of the movable sliding plate (5) that is mounted on the top of the linear thermal conduction system which is in turn covered by a jacket of Teflon rubber (15). The Teflon rubber jacket has a circular aperture at its top. A cylindrical aluminum piece of diameter 25 mm and height of 25 mm is used between the movable sliding

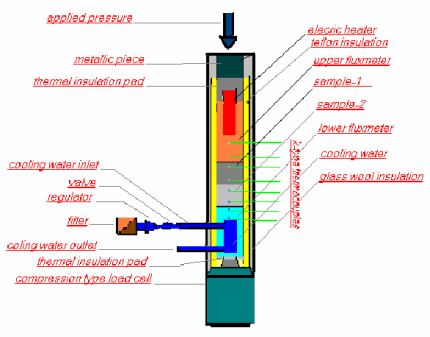

Figure 5 Schematic diagram of the setup used to measure thermal joint conductance

plate and the heating system at the top of the linear thermal conduction section. This guarantees that the Teflon rubber will not be affected by compression and that the force is applied upon the samples through the heating system. The load cell under the linear thermal conduction section responses the applied force and the

digital strain indicator indicates the compression strain which is proportional to the applied load. Details of the linear conduction system are shown in **figure 5**.

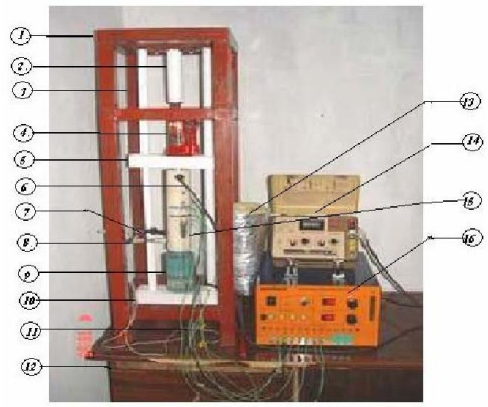

Figure 6:Experimental setup

Temperature Measuring System:

The thermocouples used to measure the temperature in the present work were of insulated core k-type. Each thermocouple was fitted with a miniature plug for direct connection to the panel of the Heat Transfer Service Unit. Eight thermocouples in total are installed, two per each of the upper and lower flux meters and upper and lower samples respectively. Thermocouples beads were located on the centerline of each section in holes at different angular positions to minimize the disturbance to heat flow along the sections as was mentioned earlier. All thermocouple readings were monitored digitally with an accuracy of $\pm 0.1^{\circ}$ C by the Heat Transfer Service Unit.

In order to check the validity of the thermocouple, the thermocouple readings is tested against a mercury thermometer for the freezing point of water ($0^{\circ}C$) and its boiling point ($100^{\circ}C$). Excellent agreement is shown between the two readings. Details of upper and lower fluxmeters, cooling system, thermal insulation, roughness measurements,hardness measurements, out-of –flatness measurements wer mentioned in [26]. Table (5.4): shows geometrical, mechanical, and thermal properties of the contacting surfaces and thermal grease.

Experimental Procedure:

In this case, samples were chemically cleaned with acetone solution to remove the dirt and oils. After that and for more cleaning an ultrasonic cleaning were used. Then samples were arranged in the system shown by figure (4.1) and all joints, except that between the two samples, were filled with thermal grease to enhance heat transfer operations.

The constant flow cooling water is turned on and the Heat Transfer Service Unit is switched on. Using the adjustable voltage control potentiometer, the heater voltage was chosen. At this time, the heater is on and the cooling water is circulating. Then the digital strain indicator is switched on and a load is applied using the hydraulic jack. As long as the temperatures of different parts of the thermal section are in variation the whole system is allowed to stabilize. In this work the experimental run may last several hours to get steady state and temperatures are stable. The steady state is established when the temperature change during three hours was $< 0.3^{\circ}$ C. When the temperatures are stable along the system, they are recorded for the eight thermocouples. Also the readings of the strain indicator were recorded. Then the applied load is increased using the hydraulic jack and the same procedures are repeated. Many runs were done for each pair of contacting samples and the different measurements were tabulated in tables (5.1) and (5.2).

In order to study the effects of using thermal greases as a thermal joint conductance enhancement, thermal grease is used as thermal interstitial material (TIM). The grease used for this purpose is RS-Heat Sink Compound. The same above procedures were repeated. The results were tabulated in table (5.3).

Experimental Data Reduction

The temperature drop across the thermal joint which is shown in **figure 7** is calculated from the following equation :

$$\Delta T_j = T_a - T_b$$

where T_a is the temperature at the lower end of the upper specimen that is to be calculated by extrapolating the straight line of temperature gradient along the upper specimen from the measurements of temperatures T_3 and T_4 at distances x_3 and x_4 from the beginning of the linear conduction section, and T_b is the temperature at the beginning of the lower specimen that is also to be calculated by extrapolating the straight line of temperature gradient along the lower specimen from the measurements of temperatures T_5 and T_6 at distances x_5 and x_6 from the beginning of the linear conduction section. The temperatures T_a and T_b are given by the following equations:

$$T_a = 1.5\,T_4 - 0.5\,T_3 \qquad T_b = 1.5\,T_5 - 0.5\,T_6. \tag{51}$$

Accordingly ΔT_j is given by the following equation:

$$\Delta T_j = 1.5(T_4 - T_5) - 0.5(T_3 - T_6) \tag{52}$$

Table (5.1) The measured applied force and along the thermal section (G_1)

Applied force	*F(N)*	1071	1919	2516	3499
Upper fluxmeter	$T_1(c^{\circ})$	73.5	69.1	69.6	67.9
	$T_2(c^{\circ})$	68.3	63.9	64.3	62.6
Upper specimen	$T_3(c^{\circ})$	60.8	57.5	57.9	56.3
	$T_4(c^{\circ})$	56.1	52.7	53.1	51.5
Lower specimen	$T_5(c^{\circ})$	47.4	47.3	47.8	46.3
	$T_6(c^{\circ})$	44.5	44.6	45.1	43.5
Lower fluxmeter	$T_7(c^{\circ})$	39.0	39.1	39.5	38.0
	$T_8(c^{\circ})$	34.9	35	35.4	33.8

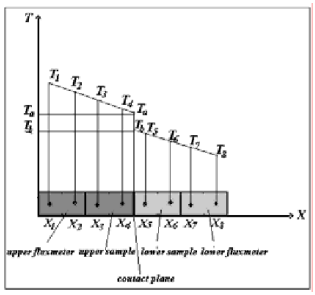

Figure 7 Schematic diagram for the temperature measured along the thermal section.

Table (5.2) The measured applied force and temperatures along the thermal section (G_2)

aApplied force	*F(N)*	647.15	1032.5	1495.01	1957.6	2593.62
Upper fluxmeter	$T_1(c^\circ)$	78.1	76.8	76.0	75.5	73.8
	$T_2(c^\circ)$	72.8	71.5	70.6	70.2	68.6
Upper specimen	$T_3(c^\circ)$	65.8	64.7	64.0	63.4	62.1
	$T_4(c^\circ)$	62.9	61.7	60.9	60.4	59.1
Lower specimen	$T_5(c^\circ)$	51.4	51.0	50.9	50.8	50.2
	$T_6(c^\circ)$	48.4	48.0	47.8	47.6	47.1
Lower fluxmeter	$T_7(c^\circ)$	40.0	40.0	39.1	39.8	39.4
	$T_8(c^\circ)$	35.7	35.6	35.4	35.2	35.2

Table (5.3) The measured applied force and temperatures along the thermal section (*G3)*

Tempe ratures *Applied force*	*F(N)*	*1032.59*	*1880*	*2689.98*	*3152.51*	*3441.59*
Upper fluxmeter	$T_1(^0c)$	*84.3*	*78.7*	*78.3*	*79.8*	*81.0*
	$T_2(^0c)$	*76.6*	*70.9*	*70.4*	*72.0*	*73.2*
Upper specimen	$T_3(^0c)$	*68.0*	*62.4*	*61.9*	*63.7*	*64.6*
	$T_4(^0c)$	*60.9*	*55.2*	*54.6*	*55.6*	*57.4*
Lower specimen	$T_5(^0c)$	*54.7*	*49.1*	*48.5*	*50.6*	*51.4*
	$T_6(^0c)$	*50.6*	*45.0*	*44.4*	*46.5*	*47.3*
Lower fluxmeter	$T_7(^0c)$	*42.0*	*36.6*	*36.0*	*38.5*	*39.2*
	$T8(^0c)$	*35.5*	*29.9*	*29.4*	*31.9*	*32.5*

The heat flux Q_j transferred through the linear thermal section is known from the calculation of the average flux through the upper and lower flux meters respectively. The thermal flux that was measured through the upper fluxmeter Q_1 and lower fluxmeter Q_2 were calculated using the Fourier heat conduction equation:

$$Q_1 = - k_U.A_U.(dT/dx)_U \quad (53)$$

$$Q_2 = - k_L.A_L.(dT/dx)_L \quad (54)$$

where k_U and k_L are thermal conductivities of the upper and lower fluxmeters, A_U and A_L are the upper and lower fluxmeters cross sections, and $(dT/dx)_U$ and $(dT/dx)_L$ are the temperature gradients along the upper and lower fluxmeters. In the present work, both of the thermal fluxmeters are of the same material and have the same cross section area, then:

$$k_U.A_U = k_L.A_L = k.A$$

and the average thermal flux can be written as:

$$Q_j = (Q_1 + Q_2)/2$$

$$Q_j = - k.A/2[(dT/dx)_U + (dT/dx)_L] \quad (55)$$

The temperature gradients in the upper and lower fluxmeters can be written as :

$$(dT/dx)_U = (T_1 - T_2)/(x_1 - x_2) \quad (56)$$

$$(dT/dx)_L = (T_7 - T_8)/(x_7 - x_8) \quad (57)$$

where T_1 and T_2 are the measured temperatures at distances x_1 and x_2 from the beginning of the linear thermal conduction section respectively, while T_7 and T_8 are the measured temperatures at distances x_7 and x_8 from the beginning of the linear thermal conduction section respectively. When, $x_1 - x_2 = x_7 - x_8 = -0.015$ m, A = 0.000491 m^2, and the fluxmeters material is Brass of k = 121 w/mk, then the final expression for R_j is written as:

$$R_j = 0.2525\left[\frac{3(T_4 - T_5) - (T_3 - T_6)}{(T_1 + T_7) - (T_2 + T_8)}\right] \quad (58)$$

The applied force is deduced from the measurement of the compression strain in the load cell by the digital stain indicator readings. When the apparent area of the contact is 0.000491m^2, the applied pressure P(MPa) is correlated to the strain as:

$$P(MPa) = 0.03924S(\mu s) + 0.18383 \quad (59)$$

Experimental Calculations

As mentioned above three experimental runs were carried out during the experimental investigation of the thermal joint conductance measurements through out part of the present work. During each run, thermal joint resistance R_j, and the external applied pressure P(MPa) where tabulated. These quantities were calculated using the experimental data of measured temperatures and the applied force tabulated in tables (5.1), (5.2), and (5.3) .

Error Analysis

Error estimation was made to the measured thermal joint resistance using the differential error analysis [27, 28]. If u_f is the amount of uncertainty in any measured quantity and that:$u_{x1}, u_{x2}, - - - - -, u_{xn}$ are the uncertainties in its independent variables, then:

$$u_f = \left[\sum_{i=1}^{n}\left(\frac{\partial f}{\partial x_i}u_{xi}\right)^2\right]^{1/2}$$

details of error analysis are mentioned in [26].

Comparing the Experimentation with Present Model

The thermal joint resistance for runs G_1 and G_2 are plotted against the applied load in **figures 8** and **9** respectively. In order to compare the measured thermal joint resistance with the modelled thermal joint resistance (equation **50**), the latter is also plotted on the same figures. Excellent agreement is shown between the measured and modelled thermal joint resistance for the cases of brass-aluminium (A_1/B_1-air) and aluminium-aluminium ($F1/D_1$- air) contacts.

Results and Discussion

The thermal joint used in the first run G_1 consists of the contact of Brass (A_1)/ Aluminium (B_1) or A_1/B_1 with air under atmospheric pressure used as TIM. Thermal joint resistance were measured in this run for four values of applied force ranging from 1071N up to 3499 N. The temperature drop across the joint ranged from 4.9 ^{0}C down to 1.4 ^{0}C. The average heat flux varies between 18.413 w and 18.8 w which can be almost regarded as constant. As a result the thermal joint resistance decreased significantly from 0.2661 ^{0}C/ w down to 0.0744 ^{0}C/ w with

error estimated to be ranged from ± 0.0055 ^{0}C/ w to ± 0.0053^{0}C/ w.

The second run G_2 was executed for the samples F_1/D_1 (Aluminum/ Aluminum) with air as TIM. The force was applied in five steps ranging from 647.15 N up to 2593.62 N. For each step the associated temperature drop was measured and it ranges from 8.55 ^{0}C down to 5.85 ^{0}C and the average heat flux was around 19 w. Throughout this run, the estimated thermal joint resistance ranges from 0.45 ^{0}C/ w down to 0.3145 ^{0}C/ w with error estimated to be ±0.0055 ^{0}C/ w. The experimental results of G_1 and G_2 are compared with the analytical model developed for the thermal joint resistance given by equation (3.80). The comparison is shown in **figures** (5.14) and (5.15) respectively. Very good agreement can be observed between them.

In order enhance the thermal joint conductance, the (Rs-Heat sink compound) thermal grease is used as TIM in run G_3. During this run, the applied force is varied in four steps ranging from 1032.59 N up to 3441.59N joint were found to be o.6 ^{0}C down to 0.35 ^{0}C. The effect of using the thermal grease (Rs-Heat sink compound) can be observed from the measured values of the thermal joint resistance that ranges from 0.02134^{0}C/ w down to 0.01219 ^{0}C w. In order to exhibit and evaluate the role of thermal joint enhancement of the thermal grease, the measured values of thermal joint conductance h_j for both was plotted against the applied force in figure (5.16). It is clear that the experimental values of the joint conductance for the joint A_1/B_1 with the thermal grease as TIM is almost 10 times its values for the joint A_1/B_1 with air as TIM (G_1) keeping all other parameters unchanged for both joints. The thermal joint conductance is calculated by equation (1.3).

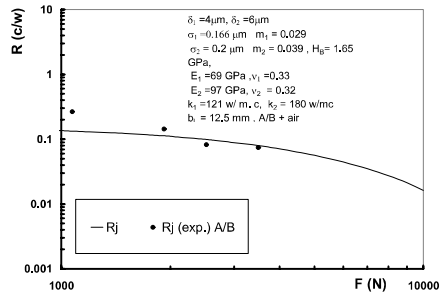

Figure 8 Comparison between the measured thermal joint resistance (A_1/B_1) the present model

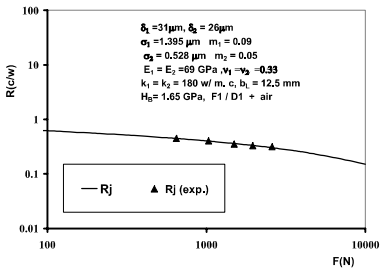

Figure 9 Comparison between the measured thermal joint resistance (F_1/D_1) and the present model.

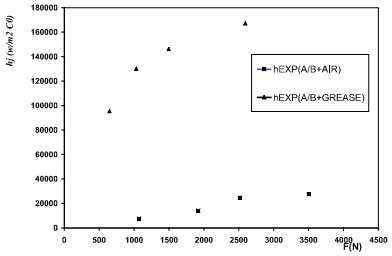

Figure 10 Comparison between the measured thermal joint conductance of the two runs G_1(without grease) and G_3 (with grease).

Table (5.4): Geometrical, mechanical, and thermal properties of the contacting surfaces and thermal grease.

Materials	*Brass* A_1	*Aluminum* B_1	*Aluminum* F_1	*Aluminum* D_1	*Thermal grease*	*Air*
σ(μm)	0.166	0.2	1.4	0.528	-----	-----
m (---)	0.029	0.04	0.09	0.05	-----	-----
δ(μm)	7	5	13	40	----	-----
b_L (*mm*)	12.5	12.5	12.5	12.5	----	-----
E (*GPa*)	97	69	69	69	----	-----
ν(---)	0.32	0.33	0.33	0.33	----	-----
H_B (*GPa*)	1.67	1.36	1.36	1.36	----	-----
k (*w/m.c*)	121	180	180	180	0.9	0.026

REFERENCES

[1] Culham, J.R., Teertstra, P., Savija, I. and Yovanovich, M.M.," Design, Assembly and Commissioning of a Test Apparatus for Characterizing Thermal Interface Materials," *Eighth Intersociety Conference on Thermal and Thermomechanical Phenomena in Electronic Systems*, San Diego, CA USA, May 29 - June 1, 2002.

[2] Johnson, K. L., "Contact Mechanics", Cambridge University Press, Cambridge, uk, 1985.

[3] Clausing, A. M., and Chao, B. T.," Thermal Contact Resistance in Vacuum Environment", *J. of Heat Transfer, vol. 87, 1965, pp. 243-251.*

[4] Mikic, b. b., and Rohsenow, W. M.," Thermal Contact Conductance" *Tech. Rep. Dep. of Mech. Eng. MIT, Cambrridge*, MA, NASA Contact NO, NGR 22-009-065, 1966,september.

[5] Yovanovich, M. R. ," Overall Constriction Resistance Between Contacting Rough, Wavy Surfaces," *Int. J. Heat Mass Transfer, vol. 12, pp. 1517-1520, 1969.*

[6] Nishino, K., Yamashita, S., and Torii, K., " Thermal Contact Conductance Under Low Applied Load in a Vacuum Environment, " *Experimental Thermal and Fluid Science, Elsevier, vol. 10, pp. 258—271, 1995.*

[7] Lambert, M. A., Fletcher L. S.," Thermal Contact Conductance of Spherical Rough Metals," *ASME J. Heat Transfer, vol. 119, no. 4, 1997, 684-690.*

[8[Bahrami, M., Yovanovich, M. M., and Culham, J. R.," Thermal Joint Resistances of Nonconforming Roughness

With Gas-Filled Gaps", *J. of Thermophysics and Heat Transfer, vol. 18, no. 3,pp.326-332, July-Sept. 2004.*
[9] Lambert, M. A.," Thermal Contact Conductance of Spherical Rough Metals", Ph.D. thesis, Texas A & M University, Dept. of Mech. Eng., College Station, TX, USA, 1995.
[10] Song, S., and Yovanovich, M. M., "Relative Contact Pressure: Dependence on Surface Roughness and Vickers Microhardness," *Journal of Thermophysics and Heat Transfer, Vol. 2, No. 1, 1988, pp. 43–47.*
[11] Sridhar, M. R., Yovanovich, M . M . " Elastoplastic Contact Conductance Model for Isotropic Uniform Rough Surfaces and Comparison with Experiment" *Trans. ASME J. Heat Transfer 1996;118:3.*
[12[Bahrami, M., " Modeling of Thermal Joint Resistance for Sphere-Flat Contact in a Vacuum", Ph.D. Thesis, University of Waterloo, 2004
[13[Milanez, F.H., Yovanovich, M.M., and Mantelli, M.B.H.," Thermal Contact Conductance at Low Contact Pressures", *Journal of Thermophysics and Heat Transfer, Vol. 18, No. 1, pp. 37-44, January-March 2004.*
[14] Cooper, M. G., Mikic, B. B., and Yovanovich, M. M. "Thermal Contact Conductance," *International Journal of Heat and Mass Transfer, vol. 12, pp. 279—300, 1969.*
[15] Mikic, B. B.," Analytical Study of Contact of Nominally Flat Surfaces: Effect of Previous Loading", *J. of Lubrication Technology, 1971, pp. 451-459.*
[16] Yovanovich, M. M. ," New Contact and Gap Conductance Correlations for Conforming Rough Surfaces" *AIAA 16th Thermophysics Conference, June 23-25, 1982/Palo Alto, California.*
[17] Antonetti, V.W. and Yovanovich, M.M., " Thermal Contact Resistance in Microelectronic Equipment ", Thermal Management Concepts in Microelectronic Packaging From Component to System, ISHM, *Technical Monograph Series 6984-003,1984,pp. 135-151.*
[18] Yovanovich, M.M., Hegazy, A.H. and DeVaal, J.W., "Surface Hardness Distribution Effects Upon Contact, Gap and Joint Conductance ", *AIAA Paper No. 82-0887, AIAA/ASME 3rd Joint Thermophysics, Fluids, Plasma and Heat Transfer Conference, St. Louis, Missouri, June 7-11, 1982, pp. 1-8.*
[19] Bahrami, M., Culham, J. R., Yovanovich, M. M., "Modeling Thermal Contact Resistance: A Scale Analysis Approach", *J. of Heat Transfer, vol. 126,pp.896-905, December 2004.*
[20] Bahrami, M. , Culham, J. R., Yovanovich, M. M., and Schneider, G. E.,"Review of Thermal Joint Resistance Models for Conforming Rough Surfaces" *Applied Mechanics Reviews, vol. 59, pp. 1-12, 2006.*
[21] Incropera, F. P., DeWitt, D. P.," Fundamentals of heat and mass transfer", 5th edition, John Wiley & Sons, Inc., USA, 2002.
[22] Negus, K . J. and Yovanovich, M. M. "Application of the Method of Optimized Images to the Steady Three Dimensional Conduction Problems," *ASME, 84-WA/HT-110, 1984.*
[23] Bahrami, M., Culham, J.R., Yovanovich, M.M. and Schneider, G.E.," Thermal Contact Resistance of Non-Conforming Rough Surfaces Part 1: Contact Mechanics Model," *AIAA Journal of Thermophysics and Heat Transfer, Vol. 18, No. 2, April-June, 2004, pp. 209-217.* Originally presented at *36th AIAA Thermophysics Conference, Orlando, Florida, June 23-26, 2003.*
[24] Hegazy, A. A., "Thermal Joint Conductance of Conforming Rough Surfaces: Effect of Surface Micro-Hardness Variation", Ph.D. thesis, University of Waterloo, Dept. of Mech. Eng., Waterloo, Canada, 1985.
[25] Yovanovich, M. M. ," Thermal –Mechanical Models for Non-Conforming Surface Contacts" Fundumentals and Applications of Conduction, May 25,2000, http:mhtl.waterloo.ca
[26] Manaf A. M.," Thermal Joint Resistance of Solid Materials as a Function of Pressure and Roughness", Ph. D Thesis, Department of Physics, College of Science, Uneversity of Mosul, Mosul, Iraq, November 2007.
[27] Ayers, G. H.," Cylindrical Thermal Contact Conductance", MSc Thesis, Texas A & M University, 2003